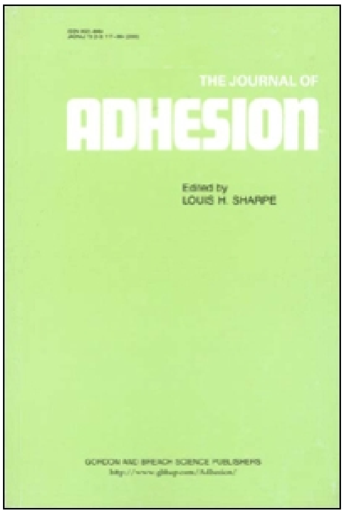

The Journal of Adhesion
Publication details, including instructions for authors and subscription information:
http://www.informaworld.com/smpp/title~content=t713453635

Characterization of Surface Pretreatments on Al/Li Alloy and Related Mechanical Properties of Polysulfone Adhesive Bonds

C. U. Ko[a]; J. P. Wightman[a]
[a] Chemistry Department, Center for Adhesion Science, Virginia Polytechnic Institute & State University, Blacksburg, VA, USA

To cite this Article Ko, C. U. and Wightman, J. P.(1987) 'Characterization of Surface Pretreatments on Al/Li Alloy and Related Mechanical Properties of Polysulfone Adhesive Bonds', The Journal of Adhesion, 24: 2, 93 — 107
To link to this Article: DOI: 10.1080/00218468708075420
URL: http://dx.doi.org/10.1080/00218468708075420

J. Adhesion, 1987, Vol. 24, pp. 93–107
Photocopying permitted by license only

Printed in the United Kingdom

Characterization of Surface Pretreatments on Al/Li Alloy and Related Mechanical Properties of Polysulfone Adhesive Bonds

C. U. KO and J. P. WIGHTMAN

Chemistry Department, Center for Adhesion Science, Virginia Polytechnic Institute & State University, Blacksburg, VA 24061, USA

(Received December 8, 1986; in final form March 2, 1987)

An investigation of polysulfone–Al/Li alloy interaction involved single lap shear joints and wedge samples following an FPL etch, sulfuric acid anodization (SAA) and phosphoric acid anodization (PAA). The study of the Al/Li surfaces involved the determination of the elemental composition and morphological features of the pretreated adherend before bonding and following fracture. When polysulfone was either thermally pressed or primed onto the microporous surface, the polysulfone indeed penetrated into the porous oxide and thereby provided a mechanical means of adhesion. The wedge test results for the adherend pretreated by PAA and SAA were superior to those for the FPL etched adherend. The failure path for the FPL etched samples was at the adhesive/oxide interface whereas the failure path for the PAA samples was within the adhesive but with occasional divergence of the crack into the oxide. The porous oxides on Al/Li alloy formed after PAA and SAA treatment were shown to undergo dramatic changes in morphology on short term (<95 hrs) exposure to 71°C and 100% R.H. environment. The mechanism of failure was due to moisture which caused hydration and subsequent weakening of the surface oxide layer and the bonded joint. Lithium was not surface concentrated in the PAA treated Al/Li alloy as shown by AES depth profiling and therefore the effect of Li on the durability of the bonded alloy is considered minimal.

KEY WORDS Polysulfone–Al/Li interface; surface pretreatments; pore penetration; oxide durability; surface characterization by XPS/STEM/AES; wedge and lap shear tests.

I INTRODUCTION

In order to characterize the adhesive bonding of a polymer–metal system, the analyses of the surface oxide and its interaction with adhesive are important. The system chosen for study is an Al/Li alloy as the adherend and polysulfone as a thermoplastic adhesive. There are a number of pretreatments which result in a porous oxide or microroughness on Al alloy surfaces.[1] Studies have indicated that when the pretreated surfaces have a porous oxide, strongly bonded joints result due to the mechanical interlocking of the adhesive with the pretreated surfaces.[2,3]

Regarding the characterization of the interaction of Al/Li oxide layer with the polysulfone, single lap shear joints and wedge samples following an FPL (Forest Products Lab) etch, sulfuric acid anodization (SAA) and phosphoric acid anodization (PAA) pretreatments were investigated. Phosphoric acid anodization (PAA) produces an oxide film on aluminum that is both porous and considerably thicker (200–400 nm) than that provided by the FPL process.[2]

In the present work, emphasis is placed on the wedge test results of polysulfone bonded Al/Li samples subjected to a hostile environment and the use of surface analysis technique to investigate the Al/Li surfaces to study the failure mechanism of bonded joints.

II EXPERIMENTAL

The Al/Li sample used in the study was Alcoa 2090 alloy having the following nominal weight percentages of minor elements: Li = 2.2; Cu = 2.7; Zr = 0.12. Polysulfone (PSF) used as a thermoplastic adhesive is UDEL P-1700 (Union Carbide). Neat PSF films (10 mil) were pressed at 290°C.

Prior to adhesive bonding of Al/Li alloy, samples were pretreated by FPL etching, SAA, and PAA. The sample is chemically etched in a sulfuric acid–sodium dichromate solution in the Forest Products Lab (FPL) pretreatment. Details of the pretreatment steps are given elsewhere.[4,5] After pretreatment of the Al/Li alloy the coupons were bonded. For both lap shear and wedge specimens, the bonding conditions were 290°C at 180 MPa (26,000 psi) for 10 minutes. The dimensions of the lap shear and wedge samples were the same as specified by ASTM.[6,7] Both the lap shear and wedge sample bonding thickness was controlled with a 0.1 mm (4 mil) wire spacer. For the wedge sample, a wedge was driven carefully with an Instron into the joint for a fixed distance and the position of the crack tip was marked. The bonded joint was placed in 71°C and 100% R.H. environment from which it was removed periodically to measure the crack tip advance. After about 140 hours of exposure, the joint was taken out and the bond pulled apart completely. Areas of the strips where environmental crack growth had occurred were then cut out for subsequent analysis.

The substrate surfaces were analysed prior to bonding and after failure of the joint by scanning transmission electron microscopy (STEM) for surface morphology, x-ray photoelectron spectroscopy (XPS), Auger electron spectroscopy (AES), and energy dispersive x-ray analysis (EDX) for surface composition. A Philips EM-420T electron microscope was used for the STEM work. Thin Al/Li samples were used and coated with about a 2 nm film of a Pd-Pt alloy. AES was done on a Perkin–Elmer PHI 610 scanning Auger microprobe. Samples were depth profiled by argon ion sputtering with a 4 kV ion beam voltage, a 25 ma emission current and a 0.2 μa ion beam current. These conditions correspond to a sputtering rate of 50 nm/min for Ta_2O_5. XPS analyses were made on a PHI 5300 ESCA system using a Mg anode.

III RESULTS AND DISCUSSION

The shear strengths of single overlap Al/Li joints not exposed to a hot-moist environment are given in Table I for the three different surface pretreated samples. The difference in lap shear strengths is minimal for all three pretreatments considering the error bars. Thus, the single lap test of samples at ambient conditions is not a good test to distinguish between surface pretreatments.

In order to distinguish between these pretreatments, the wedge

TABLE I
Shear strengths of single overlap Al/Li joints for different surface pretreatments

Pretreatment	Lap shear strength
FPL etch	19.0 ± 1.0 MPa (2770 psi)
SAA	22.0 ± 1.0 MPa (3140 psi)
PAA	25.0 ± 1.0 MPa (3670 psi)

test is utilized. One can clearly observe the difference in bond durability following different pretreatments from the crack opening wedge test as shown in Figure 1. In the case of the FPL etch treatment, the crack grew to 42 mm after being exposed to a hot-humid environment for only 30 minutes and the crack growth finally leveled off at 48 mm after 24 hours of exposure.

The SAA pretreatment resulted in improved durability over the FPL pretreatment as evidenced by a smaller crack growth which was shown to be about one-half of the FPL value. Still, a significant growth of 12 mm was observed after 1/2-hour exposure in the hot-humid environment. The crack growth leveled off at 20 mm after 24 hours of exposure. The PAA pretreatment again showed improved bond durability over the FPL etch. The crack grew to 11.5 mm after 1/2-hour exposure and then leveled off at 17.5 mm after 24 hours of exposure. The wedge test results were reproducible to within 10%.

The wedge test gives bond durability information. Since differences in rates of crack propagation between pretreatments are clearly indicated by the wedge test, then there must be differences

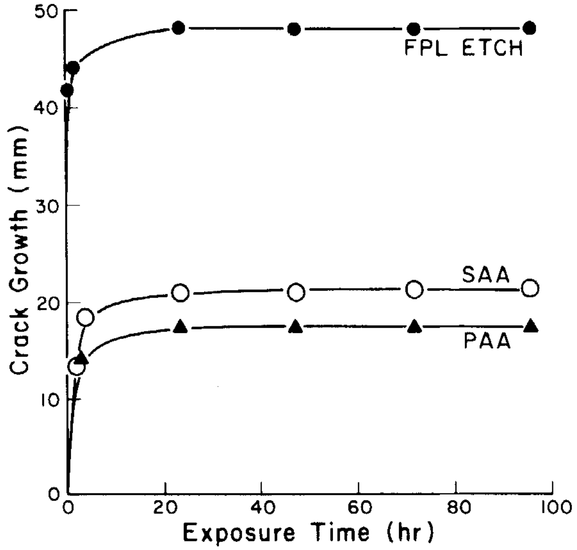

FIGURE 1 Crack growth *versus* time in 71°C and 100% R.H. environment.

in the paths of the crack propagation while the wedges were in the samples. The crack propagation depends mainly on the stability or the quality of the surface oxide, and on the polymer system used as an adhesive. Since the adhesive used was the same polysulfone in both cases, the stability of the oxide must be different to account for the durability difference observed in the wedge test. To study the Al/Li adherend surfaces prior to bonding and following fracture and to explain the difference between these pretreatments, STEM and XPS analyses were done.

A FPL etched sample

In Figure 2, the XPS C 1s and O 1s photoelectron peaks for four surfaces are shown with the binding energies (B.E.) in eV tabulated along with calculated values of the atomic percentages (A.P.).

The O 1s is photopeak assigned to aluminum oxide at 531.7 eV appears in the spectrum of the FPL etched surface. The observed S 2p peak is from the sulfuric acid used in the FPL etch solution. The Al 2p peak signal is weak from the adhesive failure side (AFS). In addition, the oxygen peak is broad and the atomic fraction of oxygen is low compared to that found on the FPL surface. The oxygen 1s photopeak is in fact a doublet resulting from two types of oxygen in polysulfone. There is a high atomic fraction of both carbon and sulfur which indicates that polysulfone used as the adhesive is attached to the AFS surface. The value of the O/S ratio of 6.5 agrees well with the value of 5.8 for neat polysulfone. The carbon and oxygen photopeaks of neat polysulfone are also included in Figure 2 for comparison.

In the spectrum of the metal failure side (MFS), the shape of the carbon and oxygen photopeaks is basically the same as seen for the pretreated FPL surface. However, S is not detected on MFS. If surface oxide is exposed, then the sulfur from sulfuric acid used in the FPL solution should be expected to be present in the top layer. The reason why sulfur is not detected is discussed below. The atomic fraction of carbon is low but the Al and O atomic fractions are high, indicating that the MFS is predominantly aluminum oxide. Therefore, the failure mode was interfacial. The absence of an Al 2p photopeak on the AFS side is additional confirmation of interfacial failure.

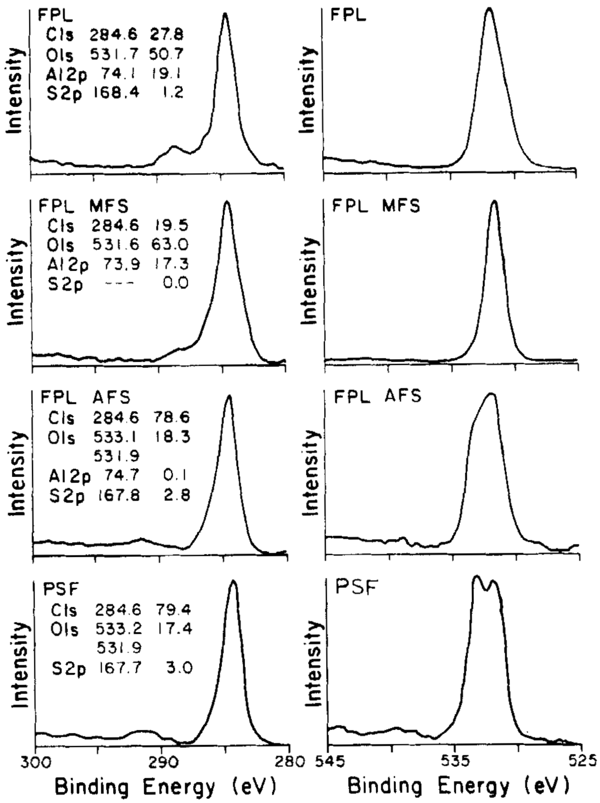

FIGURE 2 XPS spectra of C 1s and O 1s photopeaks with the binding energies in eV and atomic percentages of each element for the FPL etched surface before bonding (FPL), for the metal failure surface (MFS), for the adhesive failure surface (AFS), and for polysulfone (PSF).

Supporting evidence for the failure mode is seen in STEM micrographs. The AFS surface at 50,000 magnification is shown in Figure 3C. One can clearly see the polymer structure which was pulled away from the FPL oxide layer (see Fig. 3A). The MFS shown in Fig. 3B at 50,000 magnification shows the 'cornflake' structure as described by Venables[5] for the Al 2024 alloy. This cornflake structure is the hydroxide formed by the reaction $Al_2O_3 + H_2O \rightarrow 2\,AlOOH$; $AlOOH + H_2O \rightarrow Al(OH)_3$. The size of the cornflakes is about 200 nm. Venables[5] has observed similar hydroxide

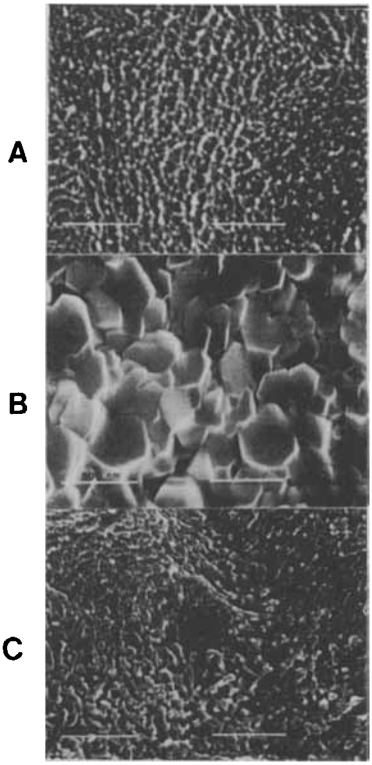

FIGURE 3 STEM photomicrographs of FPL etched (A) samples of unbonded adherend [50,000X] (B) samples of metal failure surface [50,000X] (C) samples of adhesive failure surface [50,000X].

structure with sizes of about 160 nm for the 2024 alloy. The surface aluminum oxide has become hydrated while the sample was in the 71°C and 100 % R.H. environment and the thickness of the surface layer has increased. The reason why sulfur is not detected on the MFS is due to the formation of aluminum hydroxide which covers the top surface thus preventing the S peak from being detected by XPS.

The MFS and AFS structures were representative of the whole sample indicating interfacial rather than mixed mode failure. These morphological results are in qualitative agreement with the XPS analysis reported above.

B PAA pretreated sample

The SAA pretreated and failure surfaces were very similar to the PAA pretreated and failure surfaces, therefore only PAA pretreatment is discussed. Stereo STEM photomicrographs of PAA pretreated samples before and after environmental exposure are shown in Figures 4A and 4B. At 50,000X, the surface before environmental exposure shows the fully developed whisker-like protrusion of PAA oxide with an average diameter of 100 nm into which primers and adhesives could penetrate and provide mechanical interlocking to a polymer and therefore exhibit a strong bond.

The PAA surface which was exposed to the 71°C and 100% R.H. environment for 90 hours is shown in Figure 4B. A stereo STEM photomicrograph at 25,000X reveals hydroxide structures with sizes ranging from 100 nm to 1 μm and oriented parallel to the metal surface. Therefore, as the PAA aluminum oxide is hydrated to the hydroxide, failure can occur at either the hydroxide-metal or the hydroxide-adhesive interface.

The possible penetration of polysulfone into the macropores produced by anodization of the adherend was studied by preferentially dissolving away the Al/Li alloy and the oxide, leaving the polymer for subsequent examination in the electron microscope. The stereo STEM photomicrograph of the remaining polymer

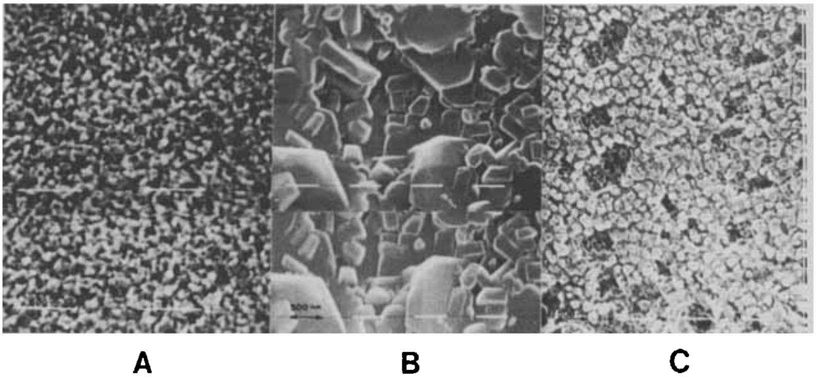

FIGURE 4 Stereo STM photomicrographs of (A) PAA samples before exposure to environment [50,000X] (B) PAA samples after exposure to environment [25,000X] (C) polymer surface after removing Al/Li alloy and its oxide layer [25,000X].

shown in Figure 4C reveals that the polysulfone had indeed penetrated into the porous oxide when thermally pressed at 290°C. The size of the polymer "cylinders" which penetrated into the macropores is 100–200 nm in diameter which corresponds to the pore size of the PAA pretreated sample. XPS results on the remaining polysulfone film confirmed that the structure observed is indeed polysulfone and not aluminum oxide. The polysulfone by itself was not affected by the aqueous 5% w/v NaOH used to dissolve Al/Li alloy and its oxide layer.

In Table II, the binding energies and atomic fractions are listed for the PAA adherends before and after exposure to the 71°C and 100 % R.H. environment as well as for the opposing failure surfaces #1 and #2 following the wedge test of PAA pretreated adherend.

The O 1s and Al 2p photopeaks assigned to the aluminum oxide at 531.3 eV and 74.2 eV, respectively, appears on both the PAA before and after exposure to the hot-humid environment. The P 2p photopeak at 133.9 eV in the spectrum of the PAA pretreated surface before environmental exposure is from the phosphoric acid. However, after environmental exposure the phosphorus peak is not observed. The reason is again due to the formation of aluminum hydroxide which covers the top surface, thus preventing P from being detected. The atomic fraction ratio of oxygen to aluminum increased from 2.04 to 3.35 after exposure to the environment. This confirms the formation of aluminum hydroxide on the PAA

TABLE II
XPS analysis of PAA Al/Li surfaces

Photopeak	PAA		PAA ENV		PAA(1)		PAA(2)	
	B.E.[a]	A.P.[b]	B.E.	A.P.	B.E.	A.P.	B.E.	A.P.
C 1s	284.6	23.0	284.6	27.0	284.6	80.0	284.6	50.0
O 1s	531.3	49.0	531.5	57.0	533.1 531.8	17.0	533.4 532.0	28.0
Al 2p	74.2	24.0	74.0	17.0	—	NSP	75.9	10.0
S 2p	—	NSP*	—	NSP	167.7	3.3	167.6	1.9
P 2p	133.9	3.2	—	NSP	—	NSP	—	NSP

[a] B.E. = binding energy (eV).
[b] A.P. = atomic percentage.
* NSP—No significant peak.

pretreated surface which had been exposed to the hot-humid environment.

On failure surface, #1, the atomic fraction of oxygen is low and the aluminum peak is not detected. However, there is a significant increase in the atomic fraction of carbon when compared to the unbonded PAA, and the sulfur peak is present at a binding energy of 167.7 eV. The sulfur peak at 167.7 eV is due to sulfur in the polysulfone adhesive. This indicates that polymer is present on failure surface #1. On failure surface #2, the higher atomic fractions of both oxygen and aluminum when compared to failure surface #1, indicates that there is some aluminum hydroxide present. Again, the atomic fraction of carbon is increased from the unbonded PAA surface and the sulfur peak is present. Both the atomic concentrations of carbon and sulfur are lower than for failure surface #1, indicating that failure surface #2 has less polymer adhesive present than failure surface #1. Therefore, the failure mode was mainly in the adhesive with the crack occasionally diverging into the surface oxide layer.

To confirm the above failure mode assignments, the STEM photomicrographs in Figures 5 and 6 were taken. Failure sample surface #1 in Figure 5A reveals the cohesively failed surface of the polymer and crack divergence into the oxide layer. At one region (see Figure 5B), hydroxide flakes can be seen having an average size of 2 μm. At another region (see Figure 5C), the polymer failure surface can be seen.

The failure surface #2 in Figure 6A shows a similar morphology to failure surface #1. However, the photomicrograph (see Fig. 6B) shows an average-sized hydroxide formation of 3 μm that stands on

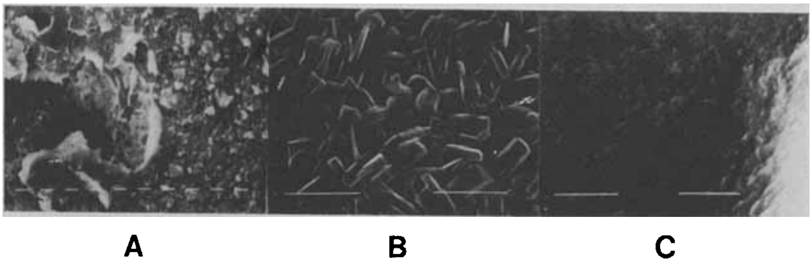

FIGURE 5 STEM photomicrographs of PAA sample of failure side #1 (A) 150X (B), 9,600X (C) 50,000X.

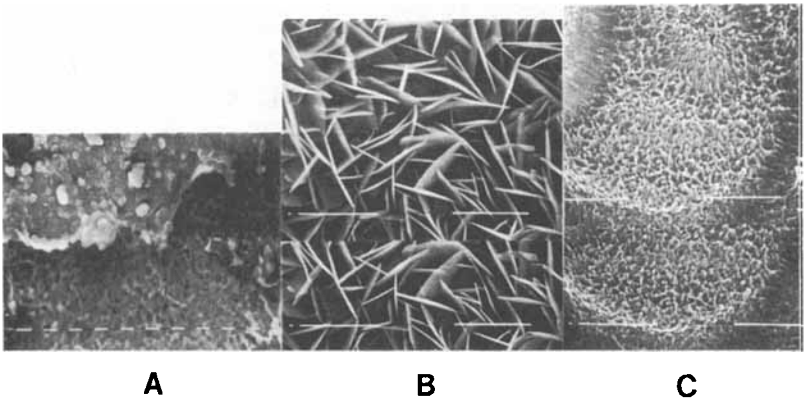

FIGURE 6 STEM photomicrograph of PAA sample of failure side #2 (A) 150X (B), 9,600X (C), 9,600X.

top of the base metal. This hydroxide flake form is quite different from the flake forms of the failure surface #1, (see Figure 5B) but is similar to that found on pretreated PAA exposed to the same hot-humid environment for 90 hours. The photomicrographs taken of the polymer side of failure surface #2 in Figure 6C show the polymer whiskers on the opposite side of the PAA oxide with whisker size of 100 nm. This may be the case where there was interfacial failure in which the polymer was simply pulled out of the pores as the wedge crack advanced. However, as discussed above, failure occurred partially within the oxide layer. The hydroxide formed on failure surface #2 differs physically from the hydroxide on failure surface #1. The EDX analysis is given in Figure 7A for the hydroxide formation on failure surface #2 of the PAA Al/Li wedge sample. Hydroxides formed on the PAA bare surface that was exposed to the 71°C and 100 % R.H. environment are shown in Figure 7B. Both of these surfaces give signals due to Al and Cu. Copper is from the Al/Li alloy which contains 2.9 % Cu as an alloying element. So it is concluded that the different morphologies of these hydroxides are not due to metal sulfates. Perhaps the difference is due to differences in crystallinity. The reason why EDX picks up Cu whereas XPS does not is that the analysis depth of EDX is 1–2 μm, much less than XPS which is only 5–10 nm, thus it does not prove the underlying metal.

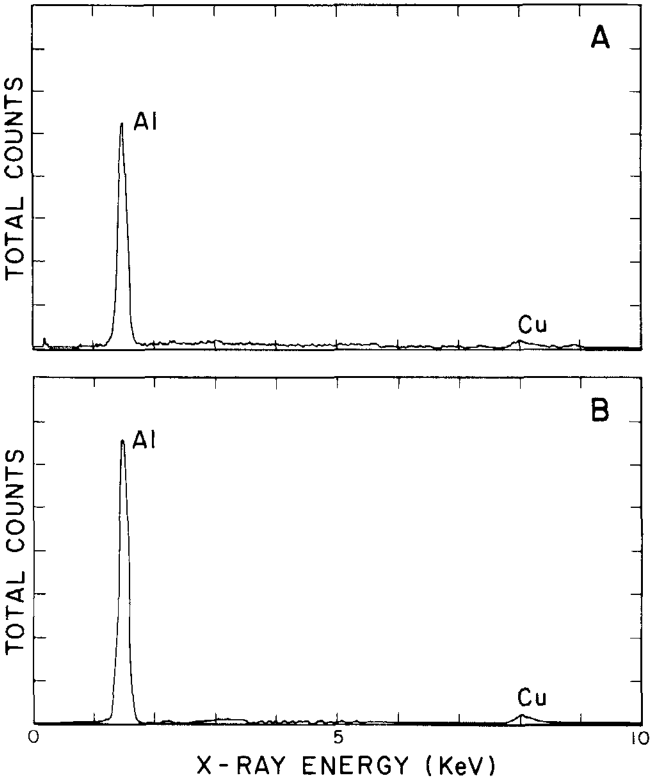

FIGURE 7 EDX result of (A) failure surface #2 of the PAA Al/Li wedge sample (B) PAA bare surface after exposure to the 71°C and 100% R.H. environment.

Therefore, the STEM micrographs confirm that the fracture mode is mainly cohesive failure within the polysulfone with the crack occasionally diverging to the oxide. Comparing the effects of the PAA to the FPL etch pretreated samples, the extent of failure within the oxide appeared to have decreased for the PAA while the degree of the cohesive fracture of the adhesive has increased. These observations are in agreement with the improved durability exhibited by the joints prepared using PAA pretreatment as indicated by the wedge test results in Figure 1.

These results have demonstrated that the mechanism of failure is due to moisture which causes hydration and subsequent weakening of the surface oxide layer. The hydration/weakening appears to occur faster for the FPL surface as compared to the PAA and SAA surfaces. The hydrated material is loosely held to the Al/Li substrate and the overall bond strength is reduced.

C Effect of Li on surface preparation by PAA (AES depth profile)

Kinloch, *et al.*,[8,9] reported that the presence of Mg on the surface is detrimental to the durability of adhesively bonded Al alloys in moist environments. In order to determine a possible similar effect of Li

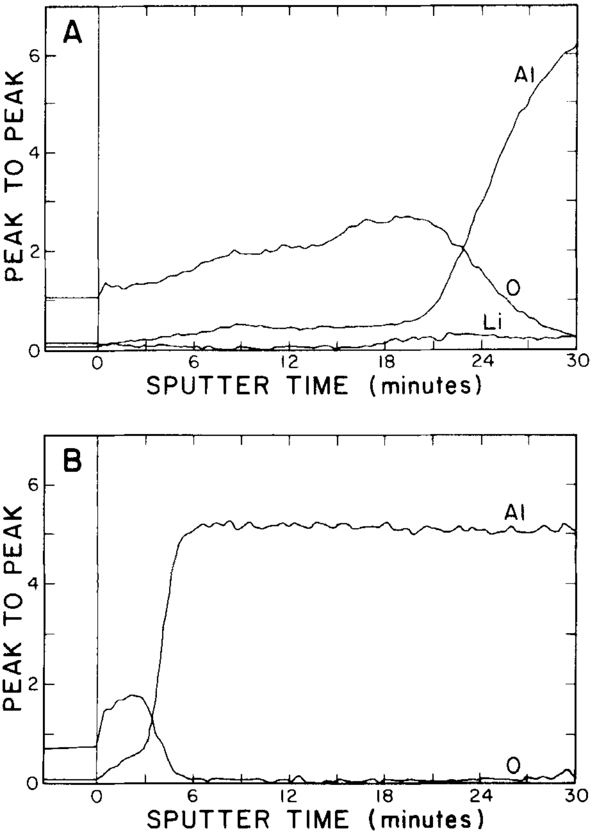

FIGURE 8 AES depth profile of (A) PAA Al/Li sample (B) PAA 2024 Al sample.

on the durability of Al/Li alloy, AES depth profiles of Al, Li and O were obtained. the peak-to-peak amplitudes of the Auger signals are plotted as a function of sputtering time in Figure 8A. Lithium is not surface concentrated as shown by the AES depth profile. Therefore, the effect of Li on the durability of the bonded alloy may be minimal. The PAA pretreated Al/Li sample has an oxide layer which takes 23 min to sputter through. The AES depth profile of Al 2024 alloy shown in Figure 8B indicates that the thickness of the oxide layer corresponds to 4 min of sputtering. Although direct comparison cannot be made between the two oxide thicknesses because of possible differences in surface roughness, surface porosity and sputtering efficiency,[10] the standard PAA treatment on the Al/Li alloy leaves a thicker oxide layer than on the 2024 Al alloy.

IV CONCLUSIONS

The goal of this study was to correlate the results of wedge tests (measured at 71°C and 100% R.H.) of FPL-etched as well as anodized surfaces before and after exposure to this hot-humid environment, with the chemical composition and the morphological features of the oxide layer on Al/Li alloy. From this investigation, the following highlights were noted:

1) Lap shear strengths of PAA and SAA pretreated Al/Li samples were slightly greater than those of FPL-etched samples.

2) Wedge test performance of PAA and SAA pretreated adherends was superior to that of the FPL-etched adherends.

3) The failure path observed with the FPL-pretreated samples was at the adhesive/oxide interface.

4) The locus of failure for the SAA and PAA samples was within the adhesive but the crack occasionally diverged into the oxide.

5) When polysulfone is thermally pressed or primed onto the microporous surface, the polysulfone indeed penetrated into the porous oxide and may have provided a mechanical means of adhesion.

6) The porous structure of anodic oxides on Al/Li formed in both sulfuric acid and phosphoric acid was shown to undergo

dramatic changes in morphology after short term (<95 hrs) exposure to 71°C and 100% R.H.

7) The morphologically different hydroxides had the same chemical composition when probed by EDX. The difference in morphologies was not due to the metal sulfates but may have been due to differences in crystallinity.

8) AES depth profile showed that Li is not surface concentrated and therefore the effect of Li on bond durability may be minimal. The oxide on Al/Li alloy was thicker than on Al 2024 alloy when the PAA pretreatment was used.

V Acknowledgements

The authors acknowledge the financial support of the Alcoa Technical Center and the Center for Innovative Technology. We thank Dr. Karl Wefers for helpful technical discussions, and Steve McCartney for assistance in the STEM work. Enabling funds for the purchase of the surface analysis equipment came from the National Science Foundation and Virginia Tech.

VI References

1. D. J. Arrowsmith and A. W. Clifford, *Intl. J. Adh. Adhesives* **3,** 193 (1983).
2. J. D. Venables, *et al., Appl. Surf. Sci.* **3,** 88 (1979).
3. D. J. Packham, in *Adhesion Aspects of Polymeric Coatings,* K. L. Mittal Ed. (Plenum, NY, 1983), pp. 18ff.
4. "Standard Practice for Preparation of Aluminum Surfaces for Structural Adhesives Bonding (Phosphoric Acid Anodizing)," ASTM D 3933-80 (1980).
5. J. D. Venables, *J. Matl. Sci.* **19,** 2431, (1984).
6. "Strength Properties of Adhesives in Shear by Tension Loading (Metal to Metal)", ASTM D1002-72 (1983).
7. "Adhesive-Bonded Surface Durability of Aluminum (Wedge Test)", ASTM D3762-79 (1983).
8. A. J. Kinloch and N. R. Smart, *J. Adhesion,* **12,** 23 (1981).
9. A. J. Kinloch, H. E. Bishop and N. R. Smart, *J. Adhesion* **14,** 105 (1982).
10. T. S. Sun, *et al., Appl. Surf. Sci.* **5,** 406 (1980).